



## Estimating the NO<sub>x</sub> produced by lightning from GOME and NLDN data: a case study in the Gulf of Mexico

S. Beirle, N. Spichtinger, A. Stohl, K. L. Cummins, T. Turner, D. Boccippio, O. R. Cooper, M. Wenig, M. Grzegorski, U. Platt, et al.

### ► To cite this version:

S. Beirle, N. Spichtinger, A. Stohl, K. L. Cummins, T. Turner, et al.. Estimating the NO<sub>x</sub> produced by lightning from GOME and NLDN data: a case study in the Gulf of Mexico. *Atmospheric Chemistry and Physics Discussions*, 2005, 5 (6), pp.11295-11329. hal-00301908

**HAL Id: hal-00301908**

**<https://hal.science/hal-00301908>**

Submitted on 18 Jun 2008

**HAL** is a multi-disciplinary open access archive for the deposit and dissemination of scientific research documents, whether they are published or not. The documents may come from teaching and research institutions in France or abroad, or from public or private research centers.

L'archive ouverte pluridisciplinaire **HAL**, est destinée au dépôt et à la diffusion de documents scientifiques de niveau recherche, publiés ou non, émanant des établissements d'enseignement et de recherche français ou étrangers, des laboratoires publics ou privés.

**Estimating lightning  
NO<sub>x</sub> from  
GOME/NLDN**

S. Beirle et al.

# Estimating the NO<sub>x</sub> produced by lightning from GOME and NLDN data: a case study in the Gulf of Mexico

**S. Beirle<sup>1</sup>, N. Spichtinger<sup>2</sup>, A. Stohl<sup>3</sup>, K. L. Cummins<sup>4</sup>, T. Turner<sup>4</sup>, D. Boccippio<sup>5</sup>, O. R. Cooper<sup>6</sup>, M. Wenig<sup>7</sup>, M. Grzegorski<sup>1</sup>, U. Platt<sup>1</sup>, and T. Wagner<sup>1</sup>**

<sup>1</sup>Institut für Umweltphysik, Universität Heidelberg, Germany

<sup>2</sup>Department of Ecology, Technical University of Munich, Germany

<sup>3</sup>Norsk institutt for luftforskning NILU, Kjeller, Norway

<sup>4</sup>Vaisala, Tucson, Arizona, USA

<sup>5</sup>Global Hydrology and Climate Center, NASA Marshall Space Flight Center, Huntsville, Alabama, USA

<sup>6</sup>NOAA Aeronomy Laboratory, Boulder, Colorado, USA

<sup>7</sup>NASA Goddard Space Flight Center, Greenbelt, Maryland, USA

Received: 12 October 2005 – Accepted: 26 October 2005 – Published: 9 November 2005

Correspondence to: S. Beirle (steffen.beirle@iup.uni-heidelberg.de)

© 2005 Author(s). This work is licensed under a Creative Commons License.

Title Page

Abstract

Introduction

Conclusions

References

Tables

Figures

◀

▶

◀

▶

Back

Close

Full Screen / Esc

Print Version

Interactive Discussion

EGU

## Abstract

Nitrogen oxides ( $\text{NO}_x = \text{NO} + \text{NO}_2$ ) play an important role in tropospheric chemistry, in particular in catalytic ozone production. Lightning provides a natural source of nitrogen oxides, dominating the production in the tropical upper troposphere, with strong impact on tropospheric ozone and the atmosphere's oxidizing capacity. Recent estimates of lightning produced  $\text{NO}_x$  ( $\text{LNO}_x$ ) are of the order of 5 Tg [N] per year with still high uncertainties in the range of one order of magnitude.

The Global Ozone Monitoring Experiment (GOME) on board the ESA-satellite ERS-2 allows the retrieval of tropospheric vertical column densities (TVCDs) of  $\text{NO}_2$  on a global scale. Here we present the GOME  $\text{NO}_2$  measurement directly over a large convective system over the Gulf of Mexico. Simultaneously, cloud-to-ground (CG) flashes are counted by the U.S. National Lightning Detection Network ( $\text{NLDN}^{\text{TM}}$ ), and extrapolated to include intra-cloud (IC)+CG flashes based on a climatological IC:CG ratio derived from NASA's space-based lightning sensors. A series of 14 GOME pixels shows largely enhanced TVCDs over thick and high clouds, coinciding with strong lightning activity. The enhancements can not be explained by transport of anthropogenic  $\text{NO}_x$  and must be due to fresh production of  $\text{LNO}_x$ . A quantitative analysis, accounting in particular for the visibility of  $\text{LNO}_x$  from satellite, yields a  $\text{LNO}_x$  production of 77 (27–230) moles of  $\text{NO}_x$ , or 1.1 (0.4–3.2) kg [N], per flash. If simply extrapolated, this corresponds to a global  $\text{LNO}_x$  production of 1.5 (0.5–4.5) Tg [N]/yr.

## 1. Introduction

Nitrogen oxides ( $\text{NO}_x = \text{NO} + \text{NO}_2$ ) play an important role in atmospheric chemistry. In the troposphere, they drive catalytic ozone production. Furthermore,  $\text{NO}_x$  controls OH concentration and thus the atmosphere's oxidizing capacity. In total, about 44 Tg [N] of nitrogen oxides are released annually, half of which are due to fossil fuel combustion (Lee et al., 1997). Further large sources are biomass burning ( $\approx 8$  Tg [N]/yr) and soil

ACPD

5, 11295–11329, 2005

## Estimating lightning $\text{NO}_x$ from GOME/NLDN

S. Beirle et al.

Title Page

Abstract

Introduction

Conclusions

References

Tables

Figures

◀

▶

◀

▶

Back

Close

Full Screen / Esc

Print Version

Interactive Discussion

EGU

emissions ( $\approx 7 \text{ Tg [N]/yr}$ ).

Lightning produced  $\text{NO}_x$  (hereafter denoted by  $\text{LNO}_x$ ) is estimated to contribute about  $5 \text{ Tg [N]/yr}$  (Lee et al., 1997). However, the best estimates of recently published studies still vary between  $0.9$  and  $12.2 \text{ Tg [N]/yr}$  (Nesbitt et al., 2000; Price et al., 1997), and the given uncertainties typically are one order of magnitude. Thus lightning is the least known important source of nitrogen oxides. Furthermore, in contrast to other sources,  $\text{LNO}_x$  is directly released also in the upper troposphere where background levels of  $\text{NO}_x$  are low and the lifetime of  $\text{NO}_x$  is about some days, i.e. several times longer than for the boundary layer ( $\approx \text{hours}$ ). Hence both tropospheric ozone as well as OH concentrations are particularly sensitive to  $\text{LNO}_x$  (e.g. Stockwell et al., 1999; Labrador et al., 2004). For the correct assessment of  $\text{NO}_x$  inventories, a prerequisite for reliable model calculations of atmospheric chemistry, better knowledge on  $\text{LNO}_x$  is essential.

Over the last decades, several studies using different methods have been performed to estimate  $\text{LNO}_x$  production. A common bottom-up approach is to assess (a) the production of  $\text{NO}_x$  per energy unit, (b) the released energy per flash and (c) the global frequency of flashes, and to estimate the global  $\text{LNO}_x$  production as the product of these quantities. Literature values range over some orders of magnitude, as a result of the many assumptions and necessary extrapolations of laboratory measurements involved (see Price et al., 1997, for an overview). Further complications arise from differences in lightning frequency as well as the relative  $\text{NO}_x$  production for cloud-to-ground (CG) and intra-cloud (IC) flashes.

In-situ measurements of  $\text{LNO}_x$  have been performed in several aircraft campaigns, where global  $\text{LNO}_x$  estimates range from  $0.9$ – $220 \text{ Tg [N]}$  per year (for overview see Huntrieser et al., 1998). In their own study, Huntrieser et al. (1998) found annual  $\text{LNO}_x$  production to be  $4$  ( $0.3$ – $22$ )  $\text{Tg [N]}$ .

Also chemical transport models (CTMs) have been used to restrict the range of  $\text{LNO}_x$  production by comparing modeled  $\text{NO}_x$  concentrations for different  $\text{LNO}_x$  scenarios with local field measurements. The studies by Levy et al. (1996), Tie et al. (2002), and

## Estimating lightning $\text{NO}_x$ from GOME/NLDN

S. Beirle et al.

Title Page

Abstract

Introduction

Conclusions

References

Tables

Figures

◀

▶

◀

▶

Back

Close

Full Screen / Esc

Print Version

Interactive Discussion

Jourdain and Hauglustaine (2001) find about 5 Tg [N], 2–6 Tg [N], and 3.5–7 Tg [N], respectively, as best estimates for yearly global LNO<sub>x</sub> production.

The fact that several independent approaches result in a global LNO<sub>x</sub> production of about 5 Tg [N] per year confirm that at least the order of magnitude can be expected to be correct. However, the uncertainties of the different methods are still quite high, indicating the need of further, independent information.

Satellite based measurements of atmospheric trace gases are a powerful addition to measurements from conventional platforms. They provide a global dataset with uniform instrumental features, and meanwhile span several years of measurements. The spectral data from the Global Ozone Monitoring Instrument GOME allow to determine column densities of various trace gases, in particular NO<sub>2</sub> (e.g. Leue et al., 2001; Richter and Burrows, 2002; Martin et al., 2002). By estimating and subtracting the stratospheric column, and accounting for radiative transfer, tropospheric NO<sub>2</sub> column densities can be derived from GOME data (e.g. Leue et al., 2001; Richter and Burrows, 2002; Beirle et al., 2003; Martin et al., 2003; Boersma et al., 2004).

The global view offered by satellite observations provides new insights on the spatial distribution of NO<sub>x</sub> sources (e.g. Velders et al., 2001; Leue et al., 2001; Richter and Burrows, 2002; Martin et al., 2003; Beirle et al., 2004b, d). The analysis of characteristic temporal and spatial patterns has been used to identify and quantify the magnitude of different NO<sub>x</sub> sources, e.g. continental anthropogenic emissions (Martin et al., 2003; Beirle et al., 2003), ship emissions (Beirle et al., 2004c; Richter et al., 2004), biomass burning (e.g. Richter and Burrows, 2002; Spichtinger et al., 2004), or soil emissions (Jaeglé et al., 2004).

On account of this successful use of GOME NO<sub>2</sub> data it is obvious to investigate LNO<sub>x</sub> from GOME as well. However, while the signal of e.g. industrial sources is often unambiguous, the clear detection of LNO<sub>x</sub> is more complex: In contrast to anthropogenic emissions, the occurrence of lightning is highly variable in space and time. Furthermore, lightning occurs predominantly in the late afternoon or evening, whereas GOME measurements take place before local noon. Due to the longer lifetime of NO<sub>x</sub>

Estimating lightning  
NO<sub>x</sub> from  
GOME/NLDN

S. Beirle et al.

Title Page

Abstract

Introduction

Conclusions

References

Tables

Figures

◀

▶

◀

▶

Back

Close

Full Screen / Esc

Print Version

Interactive Discussion

of several days in the upper troposphere (Jaegle et al., 1998),  $\text{LNO}_x$  can accumulate to detectable amounts, but these aged  $\text{LNO}_x$  plumes are diluted, and the spatial patterns are faint compared to the sharp  $\text{NO}_2$  maxima of boundary layer sources.

Moreover, thunderstorms are extreme weather events. As a consequence of deep convection and downdraft motions, the profile of lightning produced  $\text{NO}_x$  as well as  $\text{NO}_x$  from boundary layer sources is strongly modified. A large fraction of the produced  $\text{LNO}_x$  is uplifted in the anvil, resulting in a pronounced C-shaped profile of  $\text{LNO}_x$  (e.g. Pickering et al., 1998; Fehr et al., 2004). Furthermore thunderstorms are accompanied by high and thick clouds. Both factors strongly affect the visibility of  $\text{NO}_2$  from satellite.

Despite these difficulties, some studies report a correlation of lightning activity and increased  $\text{NO}_2$  column densities. Zhang et al. (2000) used  $\text{NO}_2$  data from the Upper Atmosphere Research Satellite (UARS) to substantiate a (rather qualitative) link between lightning activity and high levels of  $\text{NO}_2$  in the upper troposphere. Richter and Burrows (2002) report enhanced  $\text{NO}_2$  column densities above clouds due to lightning for Africa. Beirle et al. (2004a) analyzed correlations of monthly means of lightning activity and GOME  $\text{NO}_2$  column densities for Australia and estimated the global  $\text{LNO}_x$  production as 2.7 (0.8–14) Tg [N]/yr. Boersma et al. (2005) compared the 1997 GOME  $\text{NO}_2$  TVCDs to model output for different tropical regions and give a range for annual  $\text{LNO}_x$  production of 1.1–6.4 Tg [N]/yr.

Besides these statistical approaches, studies on particular lightning events have also been reported. Hild et al. (2000) analyzed a lightning event south from Africa coinciding with enhanced  $\text{NO}_2$  VCDs from GOME measurements nearby. Choi et al. (2005) found evidence for lightning enhancements of  $\text{NO}_2$  over North America and the western North Atlantic.

Here we present the direct GOME measurement of enhanced  $\text{NO}_2$  column densities over a large convective system in the Gulf of Mexico, while flashes are counted by the U.S. National Lightning Detection Network simultaneously.

---

**Estimating lightning  
 $\text{NO}_x$  from  
GOME/NLDN**S. Beirle et al.

---

[Title Page](#)[Abstract](#)[Introduction](#)[Conclusions](#)[References](#)[Tables](#)[Figures](#)[◀](#)[▶](#)[◀](#)[▶](#)[Back](#)[Close](#)[Full Screen / Esc](#)[Print Version](#)[Interactive Discussion](#)

## 2. Methods

### 2.1. NO<sub>2</sub> column densities from GOME

For this study we have used data from the Global Ozone Monitoring Experiment (GOME) (Burrows et al., 1999). GOME orbits the earth onboard the ERS-2 satellite, flying in a sun-synchronous nearly polar orbit and crossing the equator at 10:30 a.m. local time. The GOME instrument consists of four spectrometers measuring the radiation reflected by the earth in the UV/vis spectral range (240–790 nm) with a resolution of 0.2–0.4 nm. The extent of a GOME ground pixel is 320 km east-west and 40 km north-south (size and orientation of a GOME pixel are illustrated in Fig. 1). Within three days, global coverage is achieved at the equator.

Applying the established Differential Optical Absorption Spectroscopy (DOAS) (Platt, 1994), the GOME spectra are analyzed at 430–450 nm to derive slant column densities, i.e. integrated concentrations along the light path, of NO<sub>2</sub> (Wagner, 1999). The stratospheric fraction of the total NO<sub>2</sub> column is estimated in a reference sector over the remote Pacific (e.g. Richter and Burrows, 2002) where the tropospheric pollution is negligible. Assuming the stratospheric NO<sub>2</sub> being independent on longitude, the stratospheric column can be subtracted from the total column, resulting in tropospheric slant column densities of NO<sub>2</sub>.

The slant column densities are commonly converted to vertical column densities (VCDs), i.e. vertically integrated concentrations, via the air mass factor (AMF) (Solomon et al., 1987). The AMF (A) is defined as the ratio of SCD (S) and VCD (V), hence VCDs are derived according to

$$V=S/A. \quad (1)$$

The stratospheric AMF depends mainly on the geometric light path, i.e. the solar zenith angle. In the troposphere, the effects of Rayleigh and Mie scattering become more important. Hence tropospheric AMFs depend on the trace gas profile, the ground albedo, the aerosol load and especially on clouds. Tropospheric AMFs are derived

## Estimating lightning NO<sub>x</sub> from GOME/NLDN

S. Beirle et al.

Title Page

Abstract

Introduction

Conclusions

References

Tables

Figures

◀

▶

◀

▶

Back

Close

Full Screen / Esc

Print Version

Interactive Discussion

from radiative transfer modeling. According to Richter and Burrows (2002), Fig. 2, the tropospheric AMF at 437.5 nm is close to 1 for cloud free conditions, a homogeneous mixing in a boundary layer of 1.5 km height, maritime aerosols, and a surface albedo of 0.05. We apply the tropospheric AMFs from Richter and Burrows (2002) for the cloud free pixels of our study.

Conditions for NO<sub>2</sub> from lightning, however, are quite different: deep convection causes high and thick clouds and leads to modified vertical NO<sub>x</sub> profiles. Both factors strongly affect the NO<sub>2</sub> visibility from satellite. The calculation of appropriate AMFs for NO<sub>2</sub> from lightning in the current study is described in Sect. 4.1 in detail.

After subtraction of the stratospheric column and AMF correction, the final data products are tropospheric VCDs that are denoted with TVCDs hereafter.

## 2.2. Cloud data

Cloud information is essential for the calculation of AMFs for given satellite measurements as they shield the boundary layer, but enhance the visibility for absorbers at the cloud top due to multiple scattering and above due to the high albedo. Cloud data are retrieved on global scale from various satellite borne VIS, IR and microwave sensors. Hourly infra-red satellite images were available from the NOAA GOES-8 geostationary satellite. Channel 4 of the imager on board the satellite measures the intensity of the radiation emitted by the Earth between 10.2 and 11.2  $\mu\text{m}$ , providing the temperature of the Earth's surface and cloud tops at 4 km resolution.

In addition to data from such meteorological satellites, cloud information can be obtained from the GOME measurement itself. This has the advantage that the cloud data match the NO<sub>2</sub> observation exactly in space and time. At the IUP Heidelberg, cloud fractions are derived from intensity measurements of the polarization monitoring devices (PMDs) by the HICRU algorithm (Grzegorski et al., 2005<sup>1</sup>). The spatial PMD

<sup>1</sup>Grzegorski, M., Wenig, M., Platt, U., Stammes, P., and Wagner, T.: The Heidelberg iterative cloud retrieval utilities (HICRU) and its application to GOME data, Atmos. Chem. Phys.

## Estimating lightning NO<sub>x</sub> from GOME/NLDN

S. Beirle et al.

Title Page

Abstract

Introduction

Conclusions

References

Tables

Figures

◀

▶

◀

▶

Back

Close

Full Screen / Esc

Print Version

Interactive Discussion



resolution ( $20 \times 40 \text{ km}^2$ ) is 16 times higher than that of the GOME groundpixel. Thus HICRU provides also information on cloud heterogeneity across the GOME pixel.

### 2.3. Lightning detection: NLDN

5 The U.S. National Lightning Detection Network (NLDN<sup>TM</sup>) was the source of the archived CG lightning information. At the time of the case evaluated in this study (August 2000), the NLDN was comprised of 106 ground-based electromagnetic sensors operating in the VLF/LF frequency range. These sensors were configured to detect emissions produced by return strokes in CG lightning, and to locate these discharges using a combination of time-of-arrival and magnetic direction finding techniques (Cummins et al., 1998).  
10 The median location accuracy was 500 m, and the flash detection efficiency for events with peak current above 5 kA was estimated to be 80–90% over the continental U.S., falling off steadily out to about 500 km outside the network perimeter. Due to the fall-off of detection efficiency in the area of interest for this study, model-based corrections provided by Vaisala (Tucson, Arizona) were employed to correct for  
15 performance fall-off.

### 2.4. Transport modeling: FLEXPART

GOME measurements at a given location are “snapshots” once in 3 days. For the clear identification of  $\text{NO}_x$  sources, effects of transport have to be taken into account. In this study, transport simulations of various  $\text{NO}_x$  tracers are performed with the Lagrangian particle dispersion model FLEXPART (version 6.2) (Stohl et al., 1998, 2005) (see also  
20 <http://zardoz.nilu.no/~andreas/flextra+flexpart.html>), which simulates the transport and dispersion of non-reactive tracers by calculating the trajectories of a multitude of particles. FLEXPART was validated with data of various large scale tracer experiments (Stohl et al., 1998) and the model results were compared to different kinds of satellite

Discuss., in preparation, 2005.

## Estimating lightning $\text{NO}_x$ from GOME/NLDN

S. Beirle et al.

Title Page

Abstract

Introduction

Conclusions

References

Tables

Figures

◀

▶

◀

▶

Back

Close

Full Screen / Esc

Print Version

Interactive Discussion

data. In detail, with respect to this paper, it was already successfully used to study the advection of forest fire  $\text{NO}_x$  from Canada to Europe (Spichtinger et al., 2001), to simulate a power plant plume of  $\text{NO}_x$  traveling from South Africa towards Australia (Wenig et al., 2003), and to model the transport of anthropogenic  $\text{NO}_x$  from the US eastcoast towards Europe within a meteorological bomb (Stohl et al., 2003).

FLEXPART is driven by data from the European Centre for Medium-Range Weather Forecasts (ECMWF, 1995). The data set has a temporal resolution of 3 h (analyses at 00:00, 06:00, 12:00, and 18:00 UTC; 3-h forecasts at 03:00, 09:00, 15:00, and 21:00 UTC), a horizontal resolution of  $1^\circ \times 1^\circ$  and 60 vertical levels. Although the ECMWF model reproduces the large-scale effects of convection, they do not resolve individual deep convective cells. In order to account for subgrid-scale convection, FLEXPART was recently equipped with a convective parameterization scheme (Emanuel and Zivkovic-Rothman, 1999; Emanuel, 1991).

FLEXPART does not model chemical processes. The chemical decay of  $\text{NO}_x$  is considered by assigning the  $\text{NO}_x$  tracer with a constant e-folding lifetime. The  $\text{NO}_x$  tracer is converted into  $\text{NO}_2$  TVCDs by vertical integration and assuming a constant  $\text{NO}/\text{NO}_2$  ratio of 1. More information on the  $\text{NO}_x$  tracers simulated is given in Sect. 4.2.

### 3. Case study: a thunderstorm in the Gulf of Mexico

Lightning frequency is highest in late afternoon, while GOME measurements are taken at 10:30 a.m. local time. Nevertheless, the direct observation of lightning during an ERS-2 overpass occasionally occurs within the large amount of GOME data. An unique event of GOME capturing  $\text{LNO}_x$  just produced is found on 30 August 2000 over the Gulf of Mexico: A sequence of about 14 pixels, measured at 16:47–16:48 UTC, shows high tropospheric  $\text{NO}_2$  SCDs (Fig. 1a) and TVCDs (Fig. 1b), respectively, that by far exceed normal levels over ocean.

These high TVCDs coincide with a strong convective system causing high lightning activity. Figure 2a depicts the flashes detected by the NLDN on 30 August 2000 before

## Estimating lightning $\text{NO}_x$ from GOME/NLDN

S. Beirle et al.

Title Page

Abstract

Introduction

Conclusions

References

Tables

Figures

◀

▶

◀

▶

Back

Close

Full Screen / Esc

Print Version

Interactive Discussion

the ERS-2 overpass at 16:48 UTC. For better comparison, the GOME pixel grid is overlaid in all subplots. To illustrate the temporal coincidence of flashes and GOME measurement, Fig. 2b displays the time of the latest flash occurrence. More than half of the detected flashes occurred less than 3 h before ERS-2 overpass. Black dots indicate flashes with less than 8 min time difference to the GOME measurement.

Figure 3 shows cloud fractions (a) and cloud top temperatures (b) measured from HICRU and GOES, respectively. HICRU cloud fractions reveal a large cluster of totally clouded PMD pixels, covering an area of  $\approx 500$  km north-south and up to 300 km east-west. CTTs from GOES IR measurements at 16:15 UTC are about 200–220 K. This corresponds to cloud top heights of 12.5–16 km according to ECMWF temperature profiles.

This particular event is unprecedented as the lightning activity coincides perfectly with the GOME measurement both in space (the area affected by lightning fits in the eastern GOME pixels) and in time (most flashes have occurred during the last 3 h). The lightning event took place over sea and remote from polluted regions. The enhanced  $\text{NO}_2$  TVCDs can not be explained with transport of anthropogenic emissions (see Sect. 4.2.1). The observed enhanced  $\text{NO}_2$  TVCDs are thus unambiguously due to  $\text{LNO}_x$ . As far as we know, such a clear and direct detection of  $\text{LNO}_x$  from satellite has never been reported before.

A closer look on the meteorological situation reveals that the convective complex originates from at least two systems of different history. This is illustrated in Fig. 4 that displays hourly GOES CTTs for 30 August. Figure 4a depicts a convective cell at  $\approx 25^\circ$  N,  $85^\circ$  W, moving WSW and growing during the next hours, becoming the southern part of the large complex detected at 16:15. In fact, this system has already existed several hours before 08:15 (see the blue/cyan dots in Fig. 2b), and was even active on 29 August at the western coast of Florida.

The northern part of the 16:15 complex, however, is rather young. Tracking it back reveals that it stems from a small, singular cell emerging at about 10:15 and growing rapidly (see white marks in Figs. 4c, d, e), and some smaller systems in the north (gray

## Estimating lightning $\text{NO}_x$ from GOME/NLDN

S. Beirle et al.

Title Page

Abstract

Introduction

Conclusions

References

Tables

Figures

◀

▶

◀

▶

Back

Close

Full Screen / Esc

Print Version

Interactive Discussion

marks in f, g).

For the quantitative estimation of  $\text{LNO}_x$  given in Sect. 4, we concentrate our analysis to the northern part of the convective complex, i.e. north from  $\approx 25^\circ \text{N}$  corresponding to the GOME pixels 1–9, since the northern convection cells are young and, thus, in contrast to the southern part, free from aged  $\text{LNO}_x$ . Furthermore, the detection efficiency (DE) by NLDN is above  $\approx 30\%$  in the northern part, while it decreases to zero further south (see DE contour lines in Fig. 2a). Nevertheless, we add a discussion of the southern part also in Sect. 4.5.

#### 4. Estimate of $\text{LNO}_x$ production

We use this particular lightning event to estimate the in-situ produced  $\text{LNO}_x$ . For this task, the totally produced  $\text{NO}_x$  in the northern part of the convective complex is estimated and set in relation to the actual number of flashes.

For this quantitative analysis, the following aspects have to be discussed:

First, the sensitivity of GOME for this particular event, i.e. appropriate AMF for fresh  $\text{LNO}_x$ , will be discussed in Sect. 4.1.

Second (Sect. 4.2), the role of transport processes has to be considered.  $\text{NO}_x$  from anthropogenic sources in the USA, as well as aged  $\text{LNO}_x$  from the previous days, may be transported into the considered region and interfere with the freshly produced  $\text{LNO}_x$ . On the other hand, the fresh  $\text{LNO}_x$  may be partly transported away.

Third, the actual number of flashes has to be estimated (Sect. 4.3). The flashes detected by NLDN have to be upscaled since detection efficiency fades over sea and NLDN is insensitive for IC flashes.

Finally (Sect. 4.4), the total amount of  $\text{LNO}_x$  produced will be determined and set in relation to the total number of flashes. Our results will be compared to literature values and errors will be discussed in Sect. 5.

## Estimating lightning $\text{NO}_x$ from GOME/NLDN

S. Beirle et al.

Title Page

Abstract

Introduction

Conclusions

References

Tables

Figures

◀

▶

◀

▶

Back

Close

Full Screen / Esc

Print Version

Interactive Discussion

#### 4.1. What is the appropriate AMF for the clouded pixels?

As mentioned in Sect. 2.1, the tropospheric AMF for  $\text{NO}_2$  under usual cloud free conditions is about 1 (Richter and Burrows, 2002). This AMF is applied for the cloud free GOME pixels in Fig. 1b. But the considered GOME pixels 1–9 are covered by high and thick thunderstorm clouds that strongly impact the visibility of  $\text{NO}_2$  from GOME. Clouds have two competing effects: On the one hand,  $\text{NO}_2$  below the cloud is shielded. Especially for thick thunderstorm clouds, the boundary layer is effectively invisible from GOME. On the other hand, multiple scattering at the cloud top leads to extended light paths. Thus absorbers at the bright cloud top show an increased visibility from satellite.

For the calculation of AMFs for the clouded pixels we apply the box AMFs published by Hild et al. (2002), Fig. 3, that have been derived for cumulonimbus clouds. They thus specifically match conditions for lightning events.

The box AMFs have been calculated for  $\text{NO}_2$  layers of 1 km thickness. To derive total AMFs, these box AMFs have to be convolved with the actual trace gas profile, which is different for different  $\text{NO}_x$  sources.  $\text{NO}_x$  from ground sources, here dominated by anthropogenic emissions in the U.S., is mainly located in the boundary layer. Parts of it are lifted due to deep convection, but the fraction remaining in the lowermost kilometers is almost invisible from GOME. Taking the vertical profile derived from FLEXPART simulations for anthropogenic emissions transported to pixels 1–9 (see Sect. 4.2.1), we derive an overall AMF of 0.17 for anthropogenic  $\text{NO}_x$ .

The situation is different for  $\text{NO}_x$  from lightning:  $\text{LNO}_x$  is directly released in the free troposphere, at the very places where updraft takes place. As a result, a large amount of  $\text{LNO}_x$  is lifted up in the thunderstorm anvil, resulting in profiles often denoted as “C-shaped” (e.g. Pickering et al., 1998; Fehr et al., 2004). For the calculation of AMFs for  $\text{LNO}_x$  we convolve the box AMFs with the  $\text{LNO}_x$  profile for tropical marine thunderstorms published by Pickering et al. (1998), Table 2. This results in an AMF of 1.63. Hence  $\text{LNO}_x$  has a high visibility due to multiple scattering at the cloud top. The profile of Pickering et al. (1998), Table 2, was retrieved as mean of three single

## Estimating lightning $\text{NO}_x$ from GOME/NLDN

S. Beirle et al.

Title Page

Abstract

Introduction

Conclusions

References

Tables

Figures

◀

▶

◀

▶

Back

Close

Full Screen / Esc

Print Version

Interactive Discussion

measurements. Taking these three profiles for the AMF calculation results in 2.27, 1.63, and 1.59, respectively. The LNO<sub>x</sub> profile published by Fehr et al. (2004) (modified to a CTH of 13 km) leads to an AMF of 1.90. As the measurements from Pickering et al. (1998) match tropical marine conditions, we take an AMF of 1.63 as best estimate with an uncertainty range from 1.5 to 2.3. The high AMFs >1.9 result for profiles having large fractions of NO<sub>x</sub> at the cloud top.

As will be shown in the next section, the high NO<sub>2</sub> TVCDs detected on 30 August cannot be explained by transport of anthropogenic emissions, but is rather due to the release of fresh LNO<sub>x</sub>. We thus apply the AMF of 1.63 (1.5–2.3) for the clouded pixels 1–9 in Fig. 1b and for our quantitative estimate.

#### 4.2. What is the impact of transport?

For a quantitative view, the role of transport of NO<sub>x</sub> has to be considered. Anthropogenic NO<sub>x</sub>, in particular from the US, may have been transported in the considered region and uplifted (Sect. 4.2.1). Also aged LNO<sub>x</sub> from lightning events of the previous days may in principle contribute to the detected NO<sub>2</sub> plume, because of the NO<sub>x</sub> lifetime of several days in the upper troposphere (Sect. 4.2.2). Finally, the produced LNO<sub>x</sub> is partly transported outside the considered area (Sect. 4.2.3).

Transport is modelled with the Lagrangian tracer model FLEXPART (see Sect. 2.4). The capability of FLEXPART to track NO<sub>x</sub> transport events has been demonstrated in several studies (Spichtinger et al., 2001; Wenig et al., 2003; Stohl et al., 2003).

##### 4.2.1. Anthropogenic emissions

The transport of NO<sub>x</sub> from anthropogenic emissions is simulated with FLEXPART using the inventory for North America compiled by Frost et al. (2005) based on the U.S. EPA NEI-99 (National Emissions Inventory, base year 1999, version 3) (U.S. EPA, 2004a). This inventory was derived at 4-km horizontal resolution from spatial surrogates (U.S. EPA, 2004b) for each U.S. county and Canadian province, and average

## Estimating lightning NO<sub>x</sub> from GOME/NLDN

S. Beirle et al.

Title Page

Abstract

Introduction

Conclusions

References

Tables

Figures

◀

▶

◀

▶

Back

Close

Full Screen / Esc

Print Version

Interactive Discussion

ozone season day (June through August) county level estimates of on-road, off-road, area, and point sources. The 4-km resolution emissions are also available through a graphics information system interface (Frost and McKeen, 2004). In FLEXPART, emissions were released on the original 4-km grid in regions with high emission densities and from the 300 largest point sources. Grid cells with low emission densities and small point sources were aggregated into lower-resolution grid cells by degrading the resolution in several steps.

The e-folding lifetime for  $\text{NO}_x$  was set to 24 h, what is a rather conservative assumption, as the lifetime of boundary layer  $\text{NO}_x$  is of the order of several hours (e.g. Martin et al., 2003; Beirle et al., 2003). The tracer (a total of 5.5 million particles) was permanently released in the box  $60^\circ\text{--}170^\circ\text{W}$  and  $25^\circ\text{--}75^\circ\text{N}$  over the time period of 25 to 30 August 2000, i.e. 5 days prior the strong lightning event. To consider the vertical transport within this convective system, FLEXPART was run with the implemented convection scheme.

Figure 5 displays the resulting distribution of anthropogenic  $\text{NO}_2$  TVCDs, both in ECMWF resolution of  $1^\circ \times 1^\circ$  (Fig. 5a) as well as on GOME grid resolution (Fig. 5b). Comparison with Fig. 1b reveals that the TVCDs close to the source regions (mainly New Orleans and Houston) are overestimated in the FLEXPART run. Main reason is probably that the assumed lifetime of 24 h is too long at ground (see above) what can easily explain a factor of 2.

Over the convective complex, on the other hand, the modelled anthropogenic  $\text{NO}_x$  TVCDs are low ( $<1.3 \times 10^{15} \text{ molec/cm}^2$ ). The simulated anthropogenic  $\text{NO}_2$  TVCDs, however, seem to generally underestimate the measured  $\text{NO}_2$  TVCDs of the eastern GOME pixels. Possible reason might be that the emission inventory overestimates hot spots like New Orleans compared to the anthropogenic emissions smoothly distributed along the coast. We thus take the FLEXPART TVCD as lower limit for the actual TVCD due to anthropogenic emissions for pixels 1–9.

To derive an upper limit for the impact of anthropogenic  $\text{NO}_x$  we assume a maximum background level of anthropogenic  $\text{NO}_2$  TVCDs of  $2.5 \times 10^{15} \text{ molec/cm}^2$  over the con-

## Estimating lightning $\text{NO}_x$ from GOME/NLDN

S. Beirle et al.

Title Page

Abstract

Introduction

Conclusions

References

Tables

Figures

◀

▶

◀

▶

Back

Close

Full Screen / Esc

Print Version

Interactive Discussion



sidered area, i.e. twice as much as modelled by FLEXPART. This value corresponds to the TVCD measured by GOME north from the convective complex for cloud free conditions. Thereby, we ignore the probable decrease of anthropogenic  $\text{NO}_x$  levels southwards the coast as detected for the western and middle GOME pixels. But even  
 5 for an actual anthropogenic TVCD of  $2.5 \times 10^{15}$  molec/cm<sup>2</sup> at the eastern pixels, the expected measured TVCD would be only  $0.4 \times 10^{15}$  molec/cm<sup>2</sup>, since the strong shielding effect of the high and thick cloud cover leads to a tropospheric AMF of 0.17 for anthropogenic  $\text{NO}_2$  (see Sect. 4.1). The upper limit of anthropogenic  $\text{NO}_2$  is thus below 13% of the actually detected TVCDs, while the lower limit, taking FLEXPART TVCDs,  
 10 is half this value, i.e. 7%. We take the average, i.e. 10% as most probable value for the fraction of anthropogenic  $\text{NO}_x$ . The high  $\text{NO}_2$  TVCDs in Fig. 1a/b can thus by no means be explained with transport of anthropogenic  $\text{NO}_x$  alone.

#### 4.2.2. Aged $\text{LNO}_x$

Besides anthropogenic  $\text{NO}_x$ , aged  $\text{LNO}_x$  may contribute to the detected  $\text{NO}_2$  plume as well. In fact, NLDN detected several flashes on 29 August west from Florida. However,  
 15 as discussed in Sect. 3, part of this  $\text{LNO}_x$  is only transported to the southern part of the large complex on 30 August, while  $\text{LNO}_x$  in the northern part is freshly released.

The possible impact of aged  $\text{LNO}_x$  was estimated with FLEXPART using the NLDN flash counts from 27 August on. For every flash, a fixed amount of  $\text{NO}_2$  (artificial  
 20 units) was released in the respective grid box according to the vertical profile given by Table 2 (tropical marine) in Pickering et al. (1998). The e-folding lifetime was set to 4 days (Jaegle et al., 1998). This run was performed twice: the first run involves all flashes detected till 30 August, 16:48 UTC and stopped at 18:00 UTC (Fig. 6a). The second run simulates the same time period, but stops the release of fresh  $\text{LNO}_x$  on 30 August 00:00 UTC (Fig. 6b). I.e. run 1 shows the combination of aged and fresh  $\text{LNO}_x$ ,  
 25 while run 2 only considers aged  $\text{LNO}_x$  (i.e.  $\text{LNO}_x$  prior to 30 August). The comparison of both runs, i.e. the ratio of run 2 and run 1, allows to assess the fraction of aged  $\text{LNO}_x$ . For the  $\text{LNO}_x$  in the area covered by the GOME pixels 1–9, the fraction of aged

## Estimating lightning $\text{NO}_x$ from GOME/NLDN

S. Beirle et al.

Title Page

Abstract

Introduction

Conclusions

References

Tables

Figures

◀

▶

◀

▶

Back

Close

Full Screen / Esc

Print Version

Interactive Discussion



LNO<sub>x</sub> is 11%. It has to be noticed that this relative number depends neither on the assumptions about the LNO<sub>x</sub> released per flash nor on the DE of NLDN.

4.2.3. Outflow of LNO<sub>x</sub>

In the northern part of the convective complex, more than half of the flashes have occurred within 3 h before GOME measurement. But that also means that nearly half of the produced LNO<sub>x</sub> is older than 3 h. Parts of the LNO<sub>x</sub> produced in the area of GOME pixels 1–9 are thus transported outside. According to ECMWF windfields, main transport occurs in southerly direction. We estimate the amount of outflow using FLEXPART. Similar to the run performed in Sect. 4.1.2, the distribution of LNO<sub>x</sub> was modelled by releasing an arbitrary fixed amount of LNO<sub>x</sub> for every flash, starting from 30 August at 00:00 UTC with infinite lifetime. The resulting distribution of LNO<sub>x</sub> is compared to the hypothetical distribution of LNO<sub>x</sub> in the absence of transport, i.e. the distribution of the flash locations itself. The comparison reveals that 80% of the released LNO<sub>x</sub> remained inside the GOME pixels 1–9.

Overall, 21% of the detected NO<sub>2</sub> plume are due to anthropogenic NO<sub>x</sub> and aged LNO<sub>x</sub>, thus 79% are due to the release of fresh LNO<sub>x</sub>. To correct for the outflow of fresh LNO<sub>x</sub>, the detected NO<sub>2</sub> TVCDs have to be scaled by 100/80. Thus, in total, the measured TVCDs have to be scaled by a factor of 0.99 with an uncertainty of about 0.10 due to the different effects of transport.

4.3. How many flashes occurred?

The NLDN detects CG flashes over the US with high detection efficiency (DE). But as the measurement stations are bound to the continent, DE decreases with distance from the shore (see Fig. 2a). In the southern part of the convective complex, the estimated DE is below 5%. The clouded area (Fig. 3) reaches further south than the detected cluster of flashes (Fig. 2a), and it is very likely that flashes at the southern end are not detected at all. For pixels 1–9, however, estimated NLDN DE is above 30%. The

Estimating lightning NO<sub>x</sub> from GOME/NLDN

S. Beirle et al.

Title Page

Abstract

Introduction

Conclusions

References

Tables

Figures

◀

▶

◀

▶

Back

Close

Full Screen / Esc

Print Version

Interactive Discussion

number of flashes detected in this area is  $4.3 \times 10^4$ . Scaling this number according to the respective DE results in  $9.4 \times 10^4$  flashes.

As NLDN did not report IC flashes in 2000, this number refers to CG flashes only. To derive the total number of flashes, the number of IC flashes has to be estimated.

5 Information on the ratio of IC/CG flash frequencies can be derived from long-term comparisons of NLDN measurements with the satellite born instruments OTD (Optical Transient Detector) and LIS (Lightning Imaging Sensor) detecting both IC and CG flashes (Boccippio et al., 2000). According to the climatology for 16 July–14 October, the IC/CG ratio is 2.7 (1.8–4.0) in the considered region. I.e., the number of CG flashes

10 has to be scaled by a factor of 3.7 (2.8–5.0). Hence, we estimate the total number of flashes on 30 August 2000 in the area covered by the GOME pixels 1–9 to be  $3.49 (2.64–4.72) \times 10^5$ .

#### 4.4. What is the total quantity of $\text{LNO}_x$ produced?

The detected  $\text{NO}_2$  plume can be directly assigned to the release of fresh  $\text{LNO}_x$ . Since

15 the northern part of the convective complex is quite young (few hours), chemical decay of the produced  $\text{LNO}_x$  can be neglected due to the long lifetime of  $\text{NO}_x$  in the upper troposphere (Jaegle et al., 1998). Hence the detected  $\text{NO}_2$  TVCDs can be converted directly to the  $\text{LNO}_x$  produced.

To derive the total  $\text{NO}_2$  produced in the convective complex north from  $25^\circ \text{N}$ , the

20 respective TVCDs have to be integrated across the area of the convective system. But due to their large extent the GOME pixels cover the convective system and the cloud free, rather unpolluted ocean, at the same time. I.e. the true TVCD over the cloud is higher than the GOME TVCD that represent an average over a large area. However, this effect is quite small as the clouded part of the GOME pixel is much brighter than the

25 cloud free part, i.e. the measured light (and hence the detected absorption structures) stems from the area covered by the convective system. A quantitative estimation, given in Appendix A, leads to a correction factor of 1.2 for pixel 1, having a cloud fraction of

## Estimating lightning $\text{NO}_x$ from GOME/NLDN

S. Beirle et al.

Title Page

Abstract

Introduction

Conclusions

References

Tables

Figures

◀

▶

◀

▶

Back

Close

Full Screen / Esc

Print Version

Interactive Discussion

29%, and 1.05 on average for pixels 1–9. Hence we derive a mean corrected TVCD of  $4.24 \times 10^{15}$  molec/cm<sup>2</sup>.

5 The area of the convective system for pixels 1–9 is determined by counting the respective PMD subpixels with a HICRU CF>0.5. This results in 79 pixels of 20×40 km<sup>2</sup> each, i.e. 63 200 km<sup>2</sup> in total. Integration of the respective corrected TVCDs over the clouded area results in  $4.46 \times 10^6$  moles of NO<sub>2</sub> that are produced by this lightning event.

10 Finally, the total amount of NO<sub>2</sub> has to be extrapolated to total amount of NO<sub>x</sub>. The partitioning of NO<sub>x</sub> in NO and NO<sub>2</sub> depends on several parameters like temperature, O<sub>3</sub> concentration, and actinic flux. In the upper troposphere, most NO<sub>x</sub> is present as NO due to the low temperatures and high NO<sub>2</sub> photolysis rates. Direct measurements of the NO<sub>x</sub> partitioning within thunderstorm clouds over New Mexico have been performed by Ridley et al. (1996). Conditions for these thunderstorms are similar to the event on 30 August 2000, as they take place in August on similar latitude and close to local noon. Ridley et al. (1996), Tables 2 and 4, find a NO<sub>2</sub>/NO<sub>x</sub> ratio of about 1/6 in the anvil and upper core region. With this number,  $2.68 \times 10^7$  moles of NO<sub>x</sub> have been released by the particular lightning event in total. However, as we cannot exclude that conditions are different for the convective system under consideration, we allow a rather large range of uncertainty of 50% for the NO<sub>2</sub>/NO<sub>x</sub> ratio.

20 Combining both numbers, the total NO<sub>x</sub> release and the total number of flashes, results in a LNO<sub>x</sub> production of 77 moles/flash, or 1.1 kg [N]/flash for this particular event. Errors are discussed in detail in Sect. 5.

#### 4.5. The southern part

25 Combining measured NO<sub>2</sub> TVCDs and NLDN flash counts, we estimated the production of LNO<sub>x</sub> for pixels 1–9. This approach is not feasible for pixels 10–14 due to low NLDN DE. Nevertheless, we give a rough estimate of LNO<sub>x</sub> production for pixels 10-14 using the CTTs measured by GOES.

As lightning is caused by deep convection, flash rates have been found to be closely

## Estimating lightning NO<sub>x</sub> from GOME/NLDN

S. Beirle et al.

Title Page

Abstract

Introduction

Conclusions

References

Tables

Figures

◀

▶

◀

▶

Back

Close

Full Screen / Esc

Print Version

Interactive Discussion

related to cloud top heights (Price and Rind, 1992). We use the fraction of the GOME pixels covered by clouds with a CTT below 220 K as proxy for high clouds. This temperature corresponds to a CTH above 12.5 km. Figure 7 displays the flashes detected by NLDN (scaled accordingly to DE) in dependency of the fraction of high clouds for pixels 1–9. The correlation is  $R=0.79$ , and a linear fit (forced through zero) results in a slope of  $2.47 \times 10^4$ .

We use this relation for a simple estimate of the number of flashes for pixels 10–14, resulting in  $5.4 \times 10^4$  flashes. Taking the same factors for IC/CG ratio and  $\text{NO}_x$  partitioning as above, and neglecting transport, this results in a  $\text{LNO}_x$  production of 120 moles/flash. This number is about 50% higher than that derived for pixels 1–9. Main reason is probably an underestimation of the number of flashes for pixels 10–14, where lightning has taken place for several hours before the ERS-2 overpass (see Fig. 4), while the relation shown in Fig. 7 has been derived for the relatively young convective system covered by pixels 1–9.

## 5. Discussion

In our estimate, resulting in a  $\text{LNO}_x$  production of 77 moles/flash, several assumptions on different parameters are involved that are discussed in detail in the following. The single errors/uncertainties are not gaussian and in particular not symmetric. We thus give a conservative error range for our estimation by considering the extreme values for the effects of transport, the derived AMF, the IC/CG ratio and the  $\text{NO}_2/\text{NO}_x$  ratio. This results in a range of 27–230 moles/flash, i.e. 0.4–3.2 kg [N]/flash, for  $\text{LNO}_x$  production. Simple extrapolation, assuming a mean flash rate of 44 flashes per second globally (Christian et al., 2003), gives a global  $\text{LNO}_x$  production of 1.5 (0.5–4.5) Tg [N]/yr. This number is in good agreement with current literature values, but lower than the often cited number of 5 Tg [N]/yr. However, this particular event is not necessarily representative for global lightning.

The transport and uplift of anthropogenic  $\text{NO}_x$  has been simulated with FLEXPART

## Estimating lightning $\text{NO}_x$ from GOME/NLDN

S. Beirle et al.

Title Page

Abstract

Introduction

Conclusions

References

Tables

Figures

◀

▶

◀

▶

Back

Close

Full Screen / Esc

Print Version

Interactive Discussion

using up to date emissions and an improved convection scheme. Nevertheless, we cannot rule out that the upward transport is underestimated by FLEXPART in particular for such a rapidly evolving system. If FLEXPART underestimates the amount of anthropogenic  $\text{NO}_x$  uplifted in the anvil, we would also underestimate the AMF for anthropogenic  $\text{NO}_x$ . But on the other hand, in this case the  $\text{NO}_x$  would be shifted towards NO and the assumed NO/ $\text{NO}_2$  ratio for anthropogenic  $\text{NO}_x$  would have to be modified. For the extreme scenario of all anthropogenic  $\text{NO}_x$  lifted up and mixed homogeneously between 7 and 13 km, leading to an AMF of 1.4, and a  $\text{NO}_2/\text{NO}_x$  ratio of 1/6, anthropogenic  $\text{NO}_x$  still could only explain one fourth of the observed  $\text{NO}_2$  TCVDs.

Our quantitative estimation of  $\text{LNO}_x$  production is in particular depending on the actual AMF, the IC/CG ratio, and the  $\text{NO}_x$  partitioning. An AMF above 2.2 is quite unlikely, since this would require almost all  $\text{NO}_x$  being at the cloud top. Our AMF could be overestimated, however, if the underlying box AMFs by Hild et al. (2002) are wrong, in particular, if the true box AMFs below the cloud top decrease faster. Lower AMFs would result in a higher estimated  $\text{LNO}_x$  production and could easily lead to a factor of 2. Hence further effort has to be put on additional AMF calculations with independent models.

The climatological IC/CG ratio is a good first guess, but it has been reported in literature, that individual thunderstorms may show a very high IC/CG ratio of up to 100 (Dye et al., 2000). For such an extreme event, we would have underestimated the actual number of flashes drastically, thus overestimated the  $\text{LNO}_x$  production. However, such a scenario is rather unlikely, since the LIS measurement on 30 August, overpassing the detected convective system at 14:07–14:09 UTC, shows no increased number of flashes compared to NLDN.

The  $\text{NO}_x$  partitioning in thunderstorm clouds of geolocation, season, and local time similar to the lightning event under consideration was measured by Ridley et al. (1996). Nevertheless, we cannot exclude that the actual  $\text{NO}_x$  partitioning differs. Uncertainty is expressed by the large range of 50%, i.e. the  $\text{NO}_2/\text{NO}_x$  ratio being 1/12 up to 1/4, assumed in Sect. 4.4.

## Estimating lightning $\text{NO}_x$ from GOME/NLDN

S. Beirle et al.

Title Page

Abstract

Introduction

Conclusions

References

Tables

Figures

◀

▶

◀

▶

Back

Close

Full Screen / Esc

Print Version

Interactive Discussion

## 6. Conclusion and outlook

In past, GOME NO<sub>2</sub> data has been used to estimate LNO<sub>x</sub> production by statistical approaches (Beirle et al., 2004a; Boersma et al., 2005). The direct observation of active convective systems, however, has several advantages: Due to deep convection, the NO<sub>x</sub> is lifted up to the cloud top, where its sensitivity for satellite measurements is quite high. The LNO<sub>x</sub> plume is not yet diluted, hence local NO<sub>x</sub> levels are high. Spatial patterns can be identified and compared to flash rate patterns. And shortly after the LNO<sub>x</sub> production, its chemical loss is rather negligible, simplifying the calculation of the total NO<sub>x</sub> production.

Within this study, we could identify NO<sub>x</sub> from lightning with GOME data for a particular convective system, matching the GOME observation in space and time. The LNO<sub>x</sub> produced is estimated as 77 (27–230) moles of NO<sub>x</sub> per flash, corresponding to 1.5 (0.5–4.5) Tg [N]/yr globally. This case study impressively illustrates the fundamental feasibility of LNO<sub>x</sub> detection and quantification with satellite NO<sub>2</sub> measurements. Hence space borne spectrometers provide a new and independent approach for the estimation of LNO<sub>x</sub>.

The lightning data from NLDN is limited to the USA, where anthropogenic sources are often interfering the quantification of LNO<sub>x</sub>. The recently established World Wide Lightning Location Network WWLLN (Lay et al., 2004), as well as the long-range lightning detection networks operated by Vaisala (Pessi et al., 2004; Demetriades et al., 2005), will allow similar case studies to be carried out on a global scale and hence to fully use the potential of satellite data. Since WWLLN is partly sensitive to IC flashes, the uncertainty arising from the IC/CG ratio is also reduced.

In future, similar case studies will be performed systematically using the improved spatial resolution of the SCanning Imaging Absorption SpectroMeter for Atmospheric CHartographY SCIAMACHY, the Ozone Monitoring Instrument OMI, and the GOME successor GOME-2. Of particular interest will be the analysis of LNO<sub>x</sub> plumes from strong convective systems that are subsequently overpassed by different satel-

### Estimating lightning NO<sub>x</sub> from GOME/NLDN

S. Beirle et al.

Title Page

Abstract

Introduction

Conclusions

References

Tables

Figures

◀

▶

◀

▶

Back

Close

Full Screen / Esc

Print Version

Interactive Discussion

lite instruments, e.g. GOME-2 (09:30 a.m.), SCIAMACHY (10:00 a.m.) and OMI (01:45 p.m.). Such scenarios allow the study of LNO<sub>x</sub> plume evolution that hold – if combined with meteorological data – valuable information on LNO<sub>x</sub> profile, NO<sub>x</sub> life-time, and the LNO<sub>x</sub> produced in thunderstorms.

- 5 For the reduction of errors, it would be a milestone to have simultaneous measurements from aircraft (providing NO<sub>x</sub> profile and NO<sub>x</sub> partitioning) and satellite (capturing the whole system at once) for a strong convective complex.

Further efforts will have to be assigned to the modeling of radiative transfer and the calculation of AMFs for fresh LNO<sub>x</sub> in thunderstorm clouds.

## 10 Appendix A: Correction for partly clouded pixels

The GOME NO<sub>2</sub> measurements are taken with a rather large footprint of 320×40 km<sup>2</sup>, hence they represent mean SCDs of generally inhomogeneous NO<sub>2</sub> distributions and cloud fractions.

- 15 To estimate the SCD above the convective complex, we assume the GOME pixels being divided in a cloud free and a totally clouded part. Let *f* be the fraction of the pixel being clouded, *S*<sub>0</sub> the true SCD for the cloud free part and *S*<sub>*c*</sub> the true SCD for the clouded part of the GOME pixel. The total SCD *S* measured by GOME is the mean of *S*<sub>0</sub> and *S*<sub>*c*</sub> weighted by the area and the brightness of the cloud free and the clouded part, respectively:

$$20 \quad S = \frac{I_c \times f \times S_c + I_0 \times (1 - f) \times S_0}{I_c \times f + I_0 \times (1 - f)} \quad (A1)$$

where *I*<sub>*c*</sub> and *I*<sub>0</sub> are the intensities one would measure for a totally clouded/cloud free scene, respectively. Solving Eq. (A1) for *S*<sub>*c*</sub>, the true SCD over the clouded part is

$$S_c = S + \frac{I_0}{I_c} \times \frac{1 - f}{f} \times (S - S_0) \quad (A2)$$

## Estimating lightning NO<sub>x</sub> from GOME/NLDN

S. Beirle et al.

Title Page

Abstract

Introduction

Conclusions

References

Tables

Figures

◀

▶

◀

▶

Back

Close

Full Screen / Esc

Print Version

Interactive Discussion

The ratio  $I_0/I_c$  is gained by comparing the maximum and minimum intensities of the PMD subpixels in the blue spectral range, resulting in  $I_c \approx 7 \times I_0$ .  $S_0$  is estimated taking the SCD of the respective neighboring, cloud free center GOME pixel. With these numbers,  $S_c$  is on average higher than  $S$  by 5% for pixels 1–9. The measured SCD

5  $S$  has thus to be corrected by a factor of 1.05. The extreme cases of  $S_{0,\min}=0$  and  $S_{0,\max}=3 \times 10^{15}$  (i.e. the maximum SCD of the center GOME pixels) lead to a range of 1.04–1.10 for the correction factor.

*Acknowledgements.* This study was funded by the German Ministry for Education and Research as part of the NOXTRAM project (Atmospheric Research 2000). We would like to thank

10 the European Space Agency (ESA) operation center in Frascati (Italy) and the “Deutsches Zentrum für Luft- und Raumfahrt” DLR (Germany) for providing GOME spectra. We thank the “Deutscher Wetterdienst” for kindly providing access to ECMWF. GOES-8 satellite images were kindly provided by UNIDATA internet delivery. We thank S. A. McKeen and G. J. Frost from NOAA for making available their inventory of anthropogenic emissions in North America

15 in a format suitable for incorporation into FLEXPART.

## References

- Beirle, S., Platt, U., Wenig, M., and Wagner, T.: Weekly cycle of  $\text{NO}_2$  by GOME measurements: a signature of anthropogenic sources, *Atmos. Chem. Phys.*, 3, 2225–2232, 2003, [SRef-ID: 1680-7324/acp/2003-3-2225](#).
- 20 Beirle, S., Platt, U., Wenig, M., and Wagner, T.:  $\text{NO}_x$  production by lightning estimated with GOME, *Adv. Space Res.*, 34(4), 793–797, 2004a.
- Beirle, S., Platt, U., Wenig, M., and Wagner, T.: Highly resolved global distribution of tropospheric  $\text{NO}_2$  using GOME narrow swath mode data, *Atmos. Chem. Phys.*, 4, 1913–1924, 2004b,
- 25 [SRef-ID: 1680-7324/acp/2004-4-1913](#).
- Beirle, S., Platt, U., von Glasow, R., Wenig, M., and Wagner, T.: Estimate of nitrogen oxide emissions from shipping by satellite remote sensing, *Geophys. Res. Lett.*, 31, L18102, doi:10.1029/2004GL020312, 2004c.

## Estimating lightning $\text{NO}_x$ from GOME/NLDN

S. Beirle et al.

Title Page

Abstract

Introduction

Conclusions

References

Tables

Figures

◀

▶

◀

▶

Back

Close

Full Screen / Esc

Print Version

Interactive Discussion



- Boccippio, D. J., Cummins, K. L., Christian, H. J., and Goodman, S. J.: Combined Satellite- and Surface-Based Estimation of the Intracloud-Cloud-to-Ground Lightning Ratio over the Continental United States, *Mon. Wea. Rev.*, 129, 108–122, 2000.
- Boersma, K. F., Eskes, H. J., and Brinksma, E. J.: Error analysis for tropospheric NO<sub>2</sub> retrieval from space, *J. Geophys. Res.*, 109, D04311, doi:10.1029/2003JD003962, 2004.
- Boersma, K. F., Eskes, H. J., Meijer, E. W., and Kelder, H. M.: Estimates of lightning NO<sub>x</sub> production from GOME satellite observations, *Atmos. Chem. Phys.*, 5, 2311–2331, 2005, [SRef-ID: 1680-7324/acp/2005-5-2311](#).
- Burrows, J., Weber, M., Buchwitz, M., Rozanov, V. V., Ladstädter-Weissenmayer, A., Richter, A., de Beek, R., Hoogen, R., Bramstedt, K., Eichmann, K.-U., Eisinger, M., and Perner, D.: The Global Ozone Monitoring Experiment (GOME): Mission concept and first scientific results, *J. Atmos. Sci.*, 56, 151–175, 1999.
- Choi, Y., Wang, Y., Zeng, T., Martin, R. V., Kurosu, T. P., and Chance, K.: Evidence of light-lightning NO<sub>x</sub> and convective transport of pollutants in satellite observations over North America, *Geophys. Res. Lett.*, 32, L02805, doi:10.1029/2004GL021436, 2005.
- Christian, H. J., Blakeslee, R. J., Boccippio, D. J., Boeck, W. L., Buechler, D. E., Driscoll, K. T., Goodman, S. J., Hall, J. M., Koshak, W. J., Mach, D. M., and Stewart, M. F.: Global frequency and distribution of lightning as observed from space by the Optical Transient Detector, *J. Geophys. Res.*, 108(D1), 4005, doi:10.1029/2002JD002347, 2003.
- Cummins, K. L., Murphy, M. J., Bardo, E. A., Hiscox, W. L., Pyle, R. B., and Pifer, A. E.: A combined TOA/MDF technology upgrade of the U.S. National Lightning Detection Network, *J. Geophys. Res.*, 103(D8), 9035–9044, doi:10.1029/98JD00153, 1998.
- Demetriades, N. W. S., Murphy, M. J., and Holle, R. L.: Long range lightning nowcasting applications for meteorology, in: *World weather research program symposium*, Toulouse, France, 2005.
- Dye, J. E., Ridley, B. A., Skamarock, W., Barth, M., Venticinque, M., Defer, E., Blanchet, P., Thery, C., Laroche, P., Baumann, K., Hubler, G., Parrish, D. D., Ryerson, T., Trainer, M., Frost, G., Holloway, J. S., Matejka, T., Bartels, D., Fehsenfeld, F. C., Tuck, A., Rutledge, S. A., Lang, T., Stith, J., and Zerr, R.: An overview of the Stratospheric-Tropospheric Experiment: Radiation, Aerosols and Ozone (STERAO)-Deep Convection experiment with result from the July 10, 1996 storm, *J. Geophys. Res.*, 105, 10 023–10 045, 2000.
- ECMWF: User Guide to ECMWF Products 2.1, Meteorological Bulletin M3.2, Reading, UK, 1995.

# Estimating lightning NO<sub>x</sub> from GOME/NLDN

S. Beirle et al.

Title Page

Abstract

Introduction

Conclusions

References

Tables

Figures

◀

▶

◀

▶

Back

Close

Full Screen / Esc

Print Version

Interactive Discussion

- Emanuel, K. A.: A scheme for representing cumulus convection in large-scale models, *J. Atmos. Sci.*, 48, 2313–2335, 1991.
- Emanuel, K. A. and Zivkovic-Rothman, M.: Development and evaluation of a convection scheme for use in climate models, *J. Atmos. Sci.*, 56, 1766–1782, 1999.
- 5 Fehr, T., Höller, H., and Huntrieser, H.: Model study on production and transport of lightning-produced  $\text{NO}_x$  in a EULINOX supercell storm, *J. Geophys. Res.*, 109, D09102, doi:10.1029/2003JD003935, 2004.
- Frost, G. and McKeen, S. A.: Emission inventory mapviewer, <http://map.ngdc.noaa.gov/website/al/emissions/viewer.htm>, 2004.
- 10 Frost, G. J., McKeen, S. A., Trainer, M., Ryerson, T. B., Holloway, J. S., Sueper, D. T., Fortin, T., Parrish, D. D., Fehsenfeld, F. C., Peckham, S. E., Grell, G. A., Kowal, D., Cartwright, J., Auerbach, N., and Habermann, T.: Effects of Changing Power Plant  $\text{NO}_x$  Emissions on Ozone in the Eastern United States, *J. Geophys. Res.*, in press, 2005.
- Hild, L., Richter, A., and Burrows, J. P.: Measurements of lightning-produced  $\text{NO}_2$  by GOME and LIS, Symposium 2000 in Göteborg – Session: Atmosphere UV Radiation, Trace Gases Other Than Ozone, ID Nr. 349, 2000.
- 15 Hild, L., Richter, A., Rozanov, V., and Burrows, J. P.: Air Mass Calculations for GOME Measurements of lightning-produced  $\text{NO}_2$ , *Adv. Space Res.*, 29(11), 1685–1690, 2002.
- Huntrieser, H., Schlager, H., Feigl, C., and Höller, H.: Transport and production of  $\text{NO}_x$  in electrified thunderstorms: Survey of previous studies and new observations at midlatitudes, *J. Geophys. Res.*, 103, 28 247–28 264, 1998.
- 20 Jaeglé, L., Jacob, D. J., Wang, Y., Weinheimer, A. J., Ridley, B. A., Campos, T. L., Sachse, G. W., and Hagen, D.: Sources and chemistry of  $\text{NO}_x$  in the upper troposphere over the United States, *Geophys. Res. Lett.*, 25, 1709–1712, 1998.
- 25 Jaeglé, L., Martin, R. V., Chance, K., Steinberger, L., Kurosu, T. P., Jacob, D. J., Modi, A. I., Yoboue, V., Sigha-Nkamdjou, L., and Galy-Lacaux, C.: Satellite mapping of rain-induced nitric oxide emissions from soils, *J. Geophys. Res.*, 109, D21310, doi:10.1029/2004JD004787, 2004.
- Jourdain, L. and Hauglustaine, D.: The global distribution of lightning  $\text{NO}_x$  simulated on-line in a General Circulation Model, *Phys. Chem. Earth (C)*, 26, 585–591, 2001.
- 30 Labrador L. J., von Kuhlmann, R., and Lawrence, M. G.: Strong sensitivity of the global mean OH concentration and the tropospheric oxidizing efficiency to the source of  $\text{NO}_x$  from lightning, *Geophys. Res. Lett.*, 31, L06102, doi:10.1029/2003GL019229, 2004.

## Estimating lightning $\text{NO}_x$ from GOME/NLDN

S. Beirle et al.

Title Page

Abstract

Introduction

Conclusions

References

Tables

Figures

◀

▶

◀

▶

Back

Close

Full Screen / Esc

Print Version

Interactive Discussion

- Lay, E. H., Holzworth, R. H., Rodger, C. J., Thomas, J. N., Pinto Jr, O., and Dowden, R. L.: WWLL global lightning detection system: Regional validation study in Brazil, *Geophys. Res. Lett.*, 31(3), L03102, doi:10.1029/2003GL01888203, 2004.
- Lee, D. S., Köhler, I., Grobler, E., Rohrer, F., Sausen, R., Gallardo-Klenner, L., Olivier, J. G. J., Dentener, F. J., and Bouwman, A. F.: Estimations of global  $\text{NO}_x$  emissions and their uncertainties, *Atmos. Environ.*, 31, 1735–1749, 1997.
- Leue, C., Wenig, M., Wagner, T., Klimm, O., Platt, U., and Jähne, B.: Quantitative analysis of  $\text{NO}_2$  emissions from GOME satellite image sequences, *J. Geophys. Res.*, 106, 5493–5505, 2001.
- Levy II, H., Moxim, W. J., and Kasibhatla, P. S.: A global three-dimensional time-dependent lightning source of tropospheric  $\text{NO}_x$ , *J. Geophys. Res.*, 101(D17), 22911–22922, doi:10.1029/96JD02341, 1996.
- Martin, R. V., Chance, K., Jacob, D. J., Kurosu, T. P., Spurr, R. J. D., Bucsela, E., Gleason, J. F., Palmer, P. I., Bey, I., Fiore, A. M., Li, Q., Yantosca, R. M., and Koелеmeijer, R. B. A.: An improved retrieval of tropospheric nitrogen dioxide from GOME, *J. Geophys. Res.*, 107(D20), 4437, doi:10.1029/2001JD001027, 2002.
- Martin, R. V., Jacob, D. J., Chance, K., Kurosu, T. P., Palmer, P. I., and Evans, M. J.: Global inventory of nitrogen oxide emissions constrained by space-based observations of  $\text{NO}_2$  columns, *J. Geophys. Res.*, 108, 4537, doi:10.1029/2003JD003453, 2003.
- Nesbitt, S. W., Zhang, R., and Orville, R. E.: Seasonal and global  $\text{NO}_x$  production by lightning estimated from the Optical Transient Detector (OTD), *Tellus*, 52B, 1206–1215, 2000.
- Pessi, A., Businger, S., Cummins, K. L., and Turner, T.: On the relationship between lightning and convective rainfall over the central pacific ocean, in: ILDC 2004 18th International Lightning Detection Conference, <http://www.soest.hawaii.edu/MET/Faculty/businger/personnel/pessi/Pessi-Pacnet.doc>, ref. no. 21, Helsinki, Finland, 2004.
- Pickering, K. E., Wang, Y., Tao, W.-K., Price, C., and Müller, J.-F.: Vertical distributions of lightning  $\text{NO}_x$  for use in regional and global chemical transport models, *J. Geophys. Res.*, 103, 31203–31216, 1998.
- Platt, U.: Differential optical absorption spectroscopy (DOAS), in: *Air Monitoring by Spectrometric Techniques*, edited by: Sigrist, M., John Wiley, New York, pp. 27–84, 1994.
- Price, C. and Rind, D.: A Simple lightning parameterization for calculating global lightning distributions, *J. Geophys. Res.*, 97(D9), 9919–9933, doi:10.1029/92JD00719, 1992.
- Price, C., Penner, J., and Prather, M.,  $\text{NO}_x$  from lightning (1). Global distribution based on

## Estimating lightning $\text{NO}_x$ from GOME/NLDN

S. Beirle et al.

Title Page

Abstract

Introduction

Conclusions

References

Tables

Figures

◀

▶

◀

▶

Back

Close

Full Screen / Esc

Print Version

Interactive Discussion

- lightning physics, J. Geophys. Res., 102, 5929–5941, 1997.
- Ridley, B. A., Dye, J. E., Walega, J. G., Zheng, J., Grahek, F. E., and Rison, W.: On the production of active nitrogen by thunderstorms over New Mexico, J. Geophys. Res., 101, 20 985–21 005, 1996.
- 5 Richter, A. and Burrows, J.: Retrieval of Tropospheric NO<sub>2</sub> from GOME Measurements, Adv. Space Res., 29(11), 1673–1683, 2002.
- Richter, A., Eyring, V., Burrows, J. P., Bovensmann, H., Lauer, A., Sierk, B., and Crutzen, P. J.: Satellite measurements of NO<sub>2</sub> from international shipping emissions, Geophys. Res. Lett., 31, L23110, doi:10.1029/2004GL020822, 2004.
- 10 Solomon, S., Schmeltekopf, A. L., and Sanders, R. W.: On the interpretation of zenith sky absorption measurements, J. Geophys. Res., 92, 8311–8319, 1987.
- Spichtinger, N., Wenig, M., James, P., Platt, U., and Stohl, A.: Satellite detection of a continental-scale plume of nitrogen oxides from boreal forest fires, Geophys. Res. Lett., 28, 4579–4582, 2001.
- 15 Spichtinger, N., Damoah, R., Eckhardt, S., Forster, C., James, P., Beirle, S., Wagner, T., Novelli, P. C., and Stohl, A.: Boreal forest fires in 1997 and 1998: a seasonal comparison using transport model simulations and measurement data, Atmos. Chem. Phys., 4, 1857–1868, 2004,  
[SRef-ID: 1680-7324/acp/2004-4-1857](#).
- 20 Stockwell, D. Z., Giannakopoulos, C., Plantevin, P.-H., Carver, G. D., Chipperfield, M. P., Law, K. S., Pyle, J. A., Shallcross, D. E., and Wang, K.-Y.: Modelling NO<sub>x</sub> from lightning and its impact on global chemical fields, Atmos. Environ., 33, 4477–4493, 1999.
- Stohl, A., Hittenberger, M., and Wotawa, G.: Validation of the Lagrangian particle dispersion model FLEXPART against large scale tracer experiment data, Atmos. Environ., 32, 4245–4264, 1998.
- 25 Stohl, A., Huntrieser, H., Richter, A., Beirle, S., Cooper, O. R., Eckhardt, S., Forster, C., James, P., Spichtinger, N., Wenig, M., Wagner, T., Burrows, J. P., and Platt, U.: Rapid intercontinental air pollution transport associated with a meteorological bomb, Atmos. Chem. Phys., 3, 969–985, 2003,  
[SRef-ID: 1680-7324/acp/2003-3-969](#).
- 30 Stohl, A., Forster, C., Frank, A., Seibert, P., and Wotawa, G.: Technical note: The Lagrangian particle dispersion model FLEXPART version 6.2, Atmos. Chem. Phys., 5, 2461–2474, 2005,  
[SRef-ID: 1680-7324/acp/2005-5-2461](#).

## Estimating lightning NO<sub>x</sub> from GOME/NLDN

S. Beirle et al.

Title Page

Abstract

Introduction

Conclusions

References

Tables

Figures

◀

▶

◀

▶

Back

Close

Full Screen / Esc

Print Version

Interactive Discussion

- Tie, X., Zhang, R., Brasseur, G., and Lei, W.: Global NO<sub>x</sub> production by lightning, J. Atmos. Chem., 43, 61–74, 2002.
- U.S. EPA: EPA Clearinghouse for inventories and emissions factors: 1999 National Emission Inventory Documentation and Data – Final Version 3.0, <http://www.epa.gov/ttn/chief/net/1999inventory.html>, 2004a.
- U.S. EPA: EPA Clearinghouse for inventories and emissions factors: Related Spatial Allocation Files – “New” Surrogates; <http://www.epa.gov/ttn/chief/emch/spatial/newsurrogate.html>, 2004b.
- Velders, G. J. M., Granier, C., Portmann, R. W., Pfeilsticker, K., Wenig, M., Wagner, T., Platt, U., Richter, A., and Burrows, J.: Global tropospheric NO<sub>2</sub> column distributions: Comparing 3-D model calculations with GOME measurements, J. Geophys. Res., 106, 12 643–12 660, 2001.
- Wagner, T.: Satellite observations of atmospheric halogen oxides, PhD thesis, University of Heidelberg, <http://www.ub.uni-heidelberg.de/archiv/539>, 1999.
- Wenig, M., Spichtinger, N., Stohl, A., Held, G., Beirle, S., Wagner, T., Jähne, B., and Platt, U.: Intercontinental transport of nitrogen oxide pollution plumes, Atmos. Chem. Phys., 3, 387–393, 2003, [SRef-ID: 1680-7324/acp/2003-3-387](http://www.atmos-chem-phys.net/3/387/2003/acp/2003-3-387/).
- Zhang, R., Sanger, N. T., Orville, R. E., Tie, X., Randel, W., and Williams, E. R.: Enhanced NO<sub>x</sub> by lightning in the upper troposphere and lower stratosphere inferred from the UARS global NO<sub>2</sub> measurements, Geophys. Res. Lett., 27, 685–688, 2000.

## Estimating lightning NO<sub>x</sub> from GOME/NLDN

S. Beirle et al.

Title Page

Abstract

Introduction

Conclusions

References

Tables

Figures

◀

▶

◀

▶

Back

Close

Full Screen / Esc

Print Version

Interactive Discussion

# Estimating lightning NO<sub>x</sub> from GOME/NLDN

S. Beirle et al.

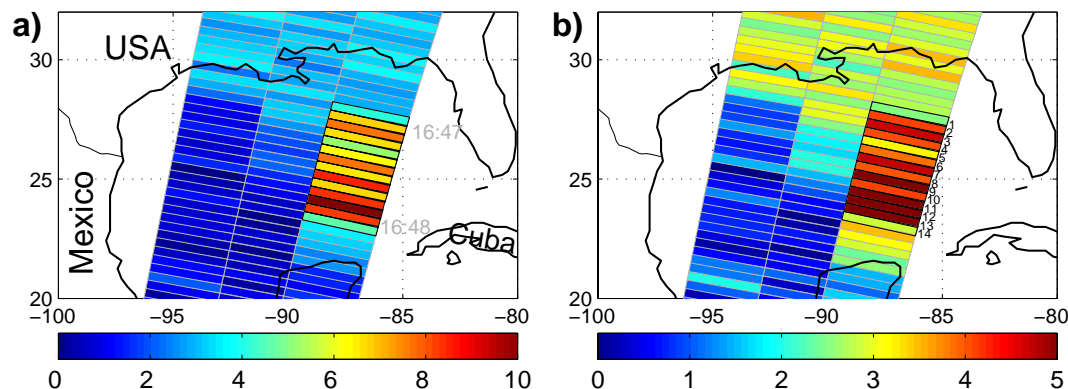


**Fig. 1.** GOME NO<sub>2</sub> observations on 30 August 2000 in the Gulf of Mexico.

**(a)** Tropospheric NO<sub>2</sub> SCDs ( $10^{15}$  molec/cm<sup>2</sup>). From 16:47–16:48, a series of 14 eastern pixels (marked in black and numbered in b) shows enhanced values above  $4 \times 10^{15}$  molec/cm<sup>2</sup>.

**(b)** NO<sub>2</sub> TVCD ( $10^{15}$  molec/cm<sup>2</sup>). The tropospheric AMFs are 1 for cloud free pixels (see Sect. 2.1) and 1.6 for the clouded pixels (see Sect. 4.1).

[Title Page](#)[Abstract](#)[Introduction](#)[Conclusions](#)[References](#)[Tables](#)[Figures](#)[◀](#)[▶](#)[◀](#)[▶](#)[Back](#)[Close](#)[Full Screen / Esc](#)[Print Version](#)[Interactive Discussion](#)

EGU

**Estimating lightning  
 $\text{NO}_x$  from  
GOME/NLDN**

S. Beirle et al.

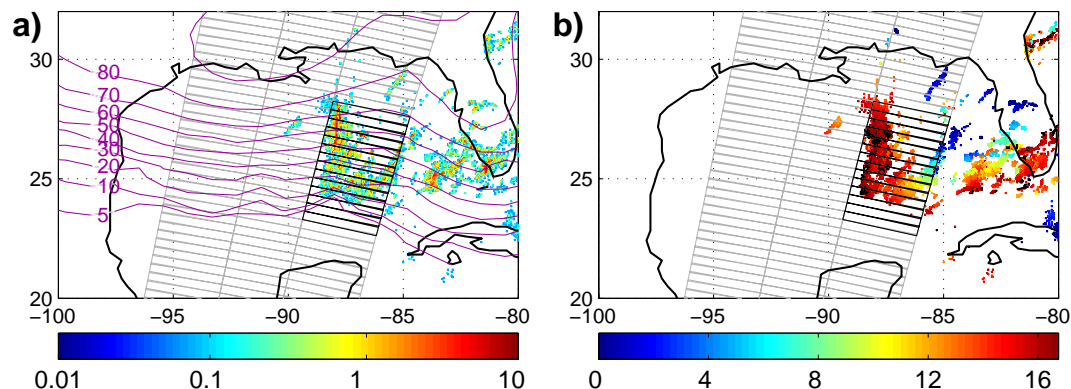


**Fig. 2.** Lightning observations on 30 August 2000 from NLDN.

**(a)** Number of detected flashes per km<sup>2</sup> before the GOME measurement. Purple contour lines display the NLDN detection efficiency. The GOME pixel grid is added as a reference for both subplots.

**(b)** Time (UTC) of the last flash detected by the NLDN previous to ERS-2 overpass (16:48). Black dots mark lightning from 16:40–16:48.

Title Page

Abstract

Introduction

Conclusions

References

Tables

Figures

◀

▶

◀

▶

Back

Close

Full Screen / Esc

Print Version

Interactive Discussion

EGU

# Estimating lightning NO<sub>x</sub> from GOME/NLDN

S. Beirle et al.

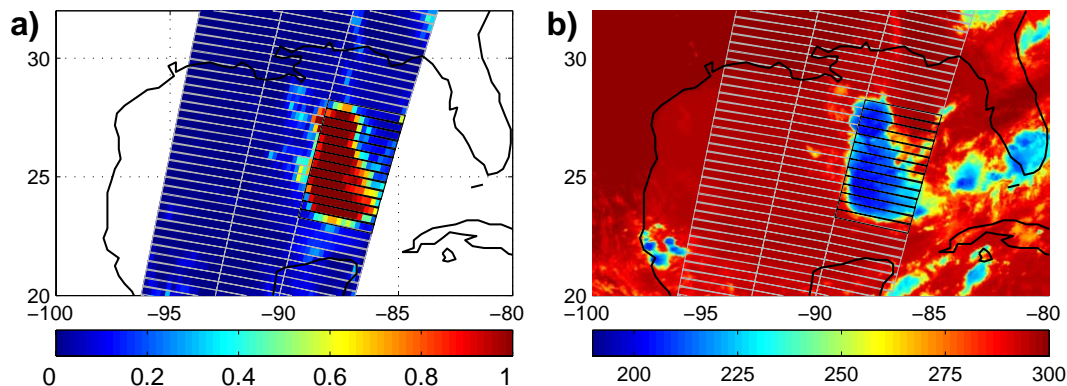


**Fig. 3.** Cloud observations on 30 August 2000.

(a) Cloud fraction derived from GOME PMD measurements (HICRU).

(b) Cloud top temperature (K) from IR measurements (GOES) at 16:15 UTC. The temperatures <220 (210) K correspond to cloud top heights >12.5 (14) km. The GOME pixel grid is added as a reference.

[Title Page](#)[Abstract](#)[Introduction](#)[Conclusions](#)[References](#)[Tables](#)[Figures](#)[◀](#)[▶](#)[◀](#)[▶](#)[Back](#)[Close](#)[Full Screen / Esc](#)[Print Version](#)[Interactive Discussion](#)

EGU



# Estimating lightning NO<sub>x</sub> from GOME/NLDN

S. Beirle et al.

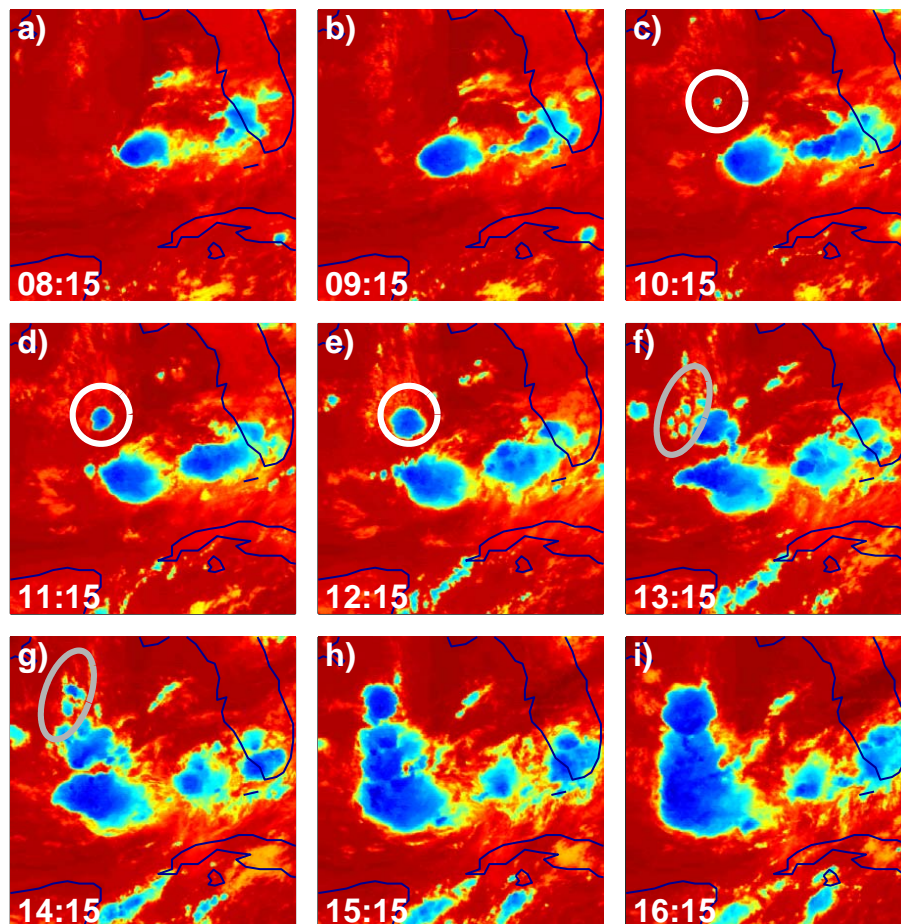


**Fig. 4.** Evolution of the convective complex as monitored by GOES CTT measurements (all times UTC). Color scale as in Fig. 3b. While the southern part (south from 25° N) has a history of several hours, the northern part just established around 10 a.m. (white marks in **c**, **d**, **e**) and after 1 p.m. (gray marks in **f**, **g**).

[Title Page](#)[Abstract](#)[Introduction](#)[Conclusions](#)[References](#)[Tables](#)[Figures](#)[◀](#)[▶](#)[◀](#)[▶](#)[Back](#)[Close](#)[Full Screen / Esc](#)[Print Version](#)[Interactive Discussion](#)

# Estimating lightning NO<sub>x</sub> from GOME/NLDN

S. Beirle et al.

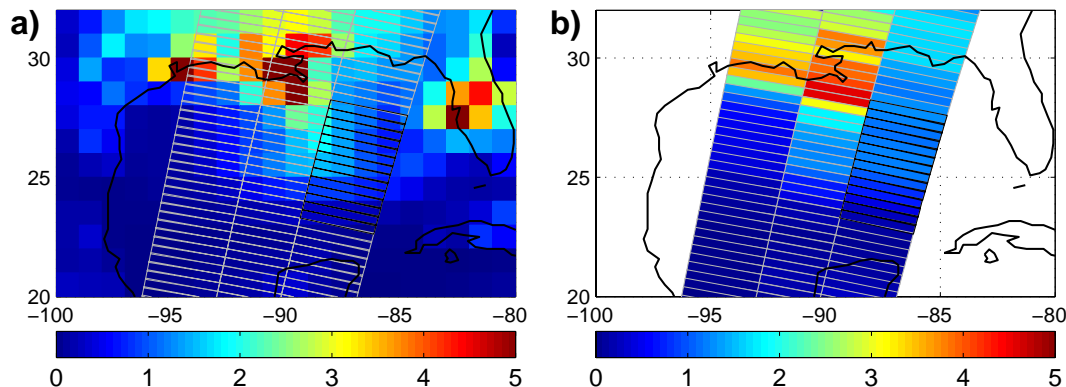


**Fig. 5. (a)** Anthropogenic NO<sub>2</sub> TVCD (10<sup>15</sup> molec/cm<sup>2</sup>) as modelled with FLEXPART, assuming a NO<sub>x</sub>-lifetime of 24 h and taking emissions from Frost et al. (2005). The GOME pixel grid is indicated as reference.

**(b)** Same as (a), but FLEXPART results are regridged on GOME grid for direct comparison with Fig. 1b.

[Title Page](#)[Abstract](#)[Introduction](#)[Conclusions](#)[References](#)[Tables](#)[Figures](#)[◀](#)[▶](#)[◀](#)[▶](#)[Back](#)[Close](#)[Full Screen / Esc](#)[Print Version](#)[Interactive Discussion](#)

EGU

# Estimating lightning $\text{NO}_x$ from GOME/NLDN

S. Beirle et al.

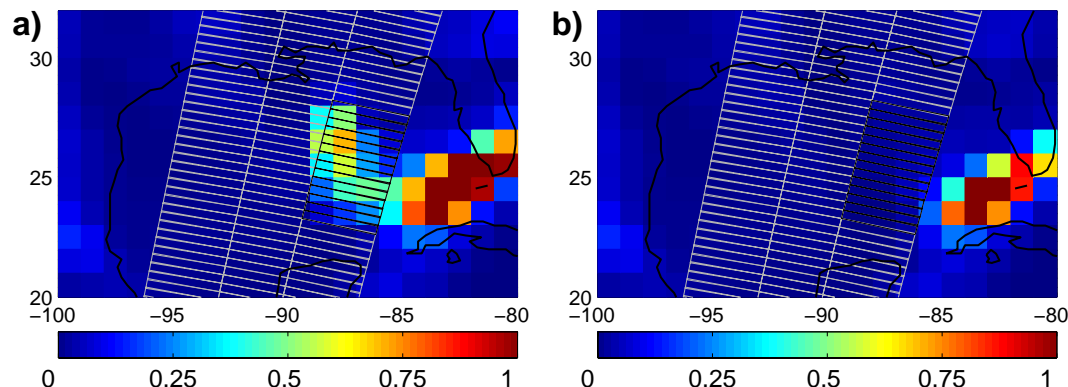


**Fig. 6.** FLEXPART simulations of  $\text{LNO}_x$  from 27 August on (artificial units). For every flash detected by NLDN, a fixed amount of  $\text{NO}_x$  was released. The  $\text{NO}_x$  lifetime was set to 4 days. Both runs are performed until 30 August, 18:00. The GOME pixel grid is added as a reference for both subplots.

**(a)** Aged plus fresh  $\text{LNO}_x$ : simulation accounts for all flashes until 30 August, 16:48.

**(b)** Aged  $\text{LNO}_x$ : simulation accounts for flashes from 27–29 August only.

For the considered GOME pixels 1–9, the fraction of aged  $\text{LNO}_x$  to total  $\text{LNO}_x$  is 11%.

[Title Page](#)[Abstract](#)[Introduction](#)[Conclusions](#)[References](#)[Tables](#)[Figures](#)[◀](#)[▶](#)[◀](#)[▶](#)[Back](#)[Close](#)[Full Screen / Esc](#)[Print Version](#)[Interactive Discussion](#)

EGU

**Estimating lightning  
NO<sub>x</sub> from  
GOME/NLDN**

S. Beirle et al.

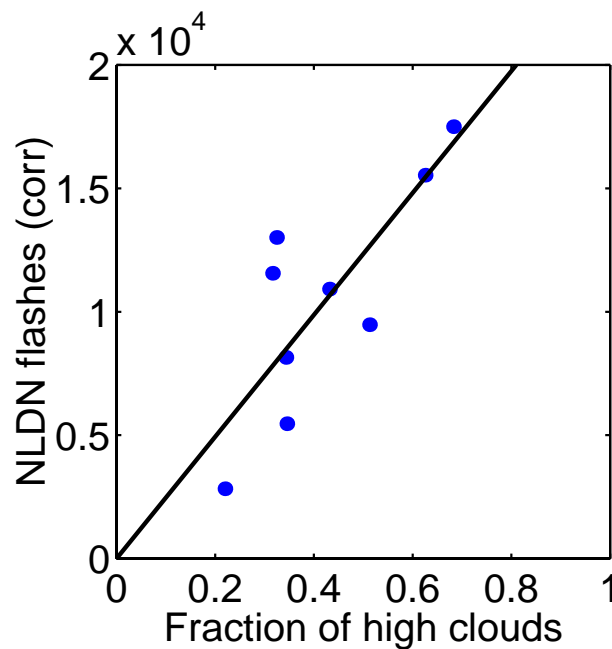


**Fig. 7.** Correlation of NLDN flash counts and the fraction of the GOME pixel covered with high clouds, i.e. having a CTT below 220 K, for pixels 1–9.

[Title Page](#)[Abstract](#)[Introduction](#)[Conclusions](#)[References](#)[Tables](#)[Figures](#)[◀](#)[▶](#)[◀](#)[▶](#)[Back](#)[Close](#)[Full Screen / Esc](#)[Print Version](#)[Interactive Discussion](#)

EGU